Geophysical Research Letters

RESEARCH LETTER
10.1029/2019GL086123

Quantification of the Uncertainty in Coastal Storm Hazard Predictions Due to Wave-Current Interaction and Wind Forcing

Charlotte E. Lyddon[1,2], Jennifer M. Brown[2], Nicoletta Leonardi[1], Andrew Saulter[3], and Andrew J. Plater[1]

[1]School of Environmental Sciences, University of Liverpool, Liverpool, UK, [2]National Oceanography Centre Liverpool, Liverpool, UK, [3]Met Office, Exeter, UK

Key Points:
- Delft3D-FLOW-WAVE is used to quantify uncertainty in water level and waves in a hypertidal estuary due to coupling and forcing processes
- Exclusion of locally generated winds underestimates significant wave height at high water by up to 90.1% in the outer estuary
- Local atmospheric forcing is vital in coastal hazard predictions for timely flood warnings and to avoid underdesigning protection schemes

Supporting Information:
- Figure S1
- Figure S2
- Figure S3
- Table S1

Correspondence to:
C. E. Lyddon,
c.e.lyddon@liverpool.ac.uk

Citation:
Lyddon, C. E., Brown, J. M., Leonardi, N., Saulter, A., & Plater, A. J. (2019). Quantification of the uncertainty in coastal storm hazard predictions due to wave-current interaction and wind forcing. *Geophysical Research Letters*, *46*, 14,576–14,585. https://doi.org/10.1029/2019GL086123

Received 4 NOV 2019
Accepted 2 DEC 2019
Accepted article online 4 DEC 2019
Published online 17 DEC 2019

Abstract Coastal flood warning and design of coastal protection schemes rely on accurate estimations of water level and waves during hurricanes and violent storms. These estimations frequently use numerical models, which, for computational reasons, neglect the interaction between the hydrodynamic and wave fields. Here, we show that neglecting such interactions, or local effects of atmospheric forcing, causes large uncertainties, which could have financial and operational consequences because flood warnings are potentially missed or protection schemes underdesigned. Using the Severn Estuary, SW England, we show that exclusion of locally generated winds underestimates high water significant wave height by up to 90.1%, high water level by 1.5%, and hazard proxy (water level + 1/2 significant wave height) by 9.1%. The uncertainty in water level and waves is quantified using a system to model tide-surge-wave conditions, Delft3D-FLOW-WAVE in a series of eight model simulations for four historic storm events.

Plain Language Summary Coastal zones worldwide are subject to combined effects of astronomical tides, meteorological storms surges, waves, and wind during storms and hurricanes, which can lead to flooding, property damage, and casualties. Coastal communities and critical infrastructure rely on accurate water level and wave forecasts to mitigate these combined hazards. Forecasts utilize hydrodynamic numerical models, which need to accurately represent these hazards and how they interact with, and feedback to, each other. This study uses a model, Delft3D-FLOW-WAVE, to calculate how tides and waves from four historic storm events combine to contribute to water level, wave height, and hazard proxy (water level + 1/2 wave height) in the Severn Estuary, southwest England. Additional simulations are run to show how local winds can further contribute to the hazard. Results show that including locally generating winds in simulations of water level, wave height, and hazard proxy is most important for accurate representation of physical processes that contribute to coastal hazards. Excluding locally generated winds from numerical model predictions could mean that flood alerts, warnings, and evacuation orders are missed, or coastal protection schemes are underdesigned, potentially leading to more flooding.

1. Introduction

Concurrence of astronomical high tides, meteorological storm surge due to hurricanes, cyclones or midlatitude storms, energetic waves, and strong winds can cause coastal flooding, and subsequent damage to property and loss of life to some of the 600 million people estimated to live in low-lying coastal (<10 m) regions worldwide (Barnard et al., 2019; Wolf, 2009). The devastating effects of concurrent coastal hazards are well documented in hypertidal regions, where tidal range exceeds 6 m, in the Severn Estuary, UK (Sibley et al., 2015), Bay of Fundy (Greenberg et al., 2012), and Yangtze Estuary (Yin et al., 2017), as combined storm parameters can enhance high water level (HWL) and high water significant wave height (HWH_s), defined as significant wave height at the time of high water, to increase the likelihood of overtopping and subsequent inundation. Increasing coastal population and urbanization, potential future changes in storm tracks, and sea level rise means that there is a need to plan for the negative consequences of coastal hazards.

Operational storm surge and wave forecasts are important components of coastal storm hazard mitigation strategies (Tunstall et al., 2004). If operational forecasts exceed predefined threshold levels, corresponding to the minimum wave and total water level that represent a potential flood hazard (Del Río et al., 2012),

alerts, and flood warnings will be issued to detail scale, timing and location of a hazard (Lawless et al., 2016). To prevent negative consequences of forecast extreme storm events, flood warnings issued by local agencies must be accurate and timely. Operational forecasts can make use of measured and modeled meteorological and oceanic data (e.g., O'Neill et al., 2016), and outputs can be used to estimate likelihood of coastal flooding and the effect of wind, waves, and total water level on overtopping and breaching for specific flood events (Quinn et al., 2014). However, error can be introduced into operational forecasts due to model, knowledge and data uncertainty (Stephens et al., 2017). Uncertainty due to a model's ability to accurately represent physical processes or replicate interactions (e.g., Bolaños et al., 2014), lack of knowledge of interactions in a physical system, and inaccurate input parameters (e.g., temporally or spatially limited) can be introduced and propagated through the modeling chain to inundation assessments and flood warnings (Sayers et al., 2003). There is a need to understand and reduce uncertainty in operational forecasts of HWL and HWH_s that contribute to hazard assessments. Uncertainty in operational forecasts could mean flood events are underestimated or missed, which may increase the risk to coastal communities and critical infrastructure.

The accurate definition of HWL and HWH_s is also important for critical storm threshold identification for the design of cost-effective coastal protection strategies. Implementation of hard structures or nature-based solutions, which aim to mitigate the effects of HWL and HWH_s, rely on a thorough understanding of the physical processes and interactions in a region (Conger & Chang, 2019). The type and costs of new schemes largely depend on the physical conditions at the site and sensitivity of the scheme to natural processes and their interaction (Temmerman et al., 2013). Uncertainty in HWL and HWH_s may lead to incorrect hazard thresholds, as defense exceedance is most likely to occur close to the time of high water or implementation of strategies, which are not able to protect hinterlands against normal winter conditions as well as extreme storm tide conditions. Commitment to upgrading engineered structures, such as Canada's recent US$114 million pledge to upgrade 64 km of dikes and sluices in Nova Scotia (Fairclough, 2019), or implementing new strategies, for example, the new £63 million seawall at Rossall, Lancashire (Environment Agency, 2018), is based on multidisciplinary, cost-benefit analysis in areas with highest potential for protection benefits. Representative, site-specific information of HWL and HWH_s are needed to support decisions to ensure crest level and defense heights are appropriate, for effective storm hazard mitigation and resilience to future change.

1.1. Case Study

This research focuses on the Severn Estuary (Figure 1a), SW England, as an example of hypertidal and funnel shaped estuaries worldwide. The estuary has the third largest mean spring tidal range in the world, up to 12.2 m at Avonmouth due to the funneling effect (Dyer, 1995), which is also known to modulate the local wave climate (Pye & Blott, 2010). The orientation of the mouth of the estuary to the Atlantic Ocean means it is exposed to prevailing swell waves, and the large fetch (up to 6,000 km) amplifies wave driven hazards in the outer estuary. The south coastline of the estuary is dominated by energy and port infrastructure and large areas of low-lying agricultural land, highlighting the need for accurate operational forecasts in this region.

1.2. Outline of the Paper

This research quantifies the sensitivity of HWL, HWH_s, and high water hazard proxies (HWHPs) to model coupling along the Severn Estuary coastline. Hazard proxy (HP) is defined as the WL + 1/2 H_s and is used to understand the severity of a condition. Thirty-two model simulations are run in total; a series of eight model simulations are run for four events, which represent a potential hazard in Delft3D-FLOW-WAVE. The model is applied to consider waves and circulation in isolation (standalone), the influence of circulation on waves (one-way coupled), and the influence of the circulation on the waves and waves on the circulation (two-way coupled). Wind and atmospheric pressure are included on four of the eight model simulations to investigate wind influence on HWL and HWH_s during storms. Water level (WL), significant wave height (H_s), and HP are simulated to explore the sensitivity of each parameter to model coupling (section 2), and the results (section 3) quantify uncertainty introduced into the model due to the coupling and forcing processes. Before concluding in section 5, section 4 discusses the importance of locally generated winds and coupling processes in simulating H_s and HP in hypertidal estuaries, and the implications that uncertainty in storm parameters have on flood warnings and management activities.

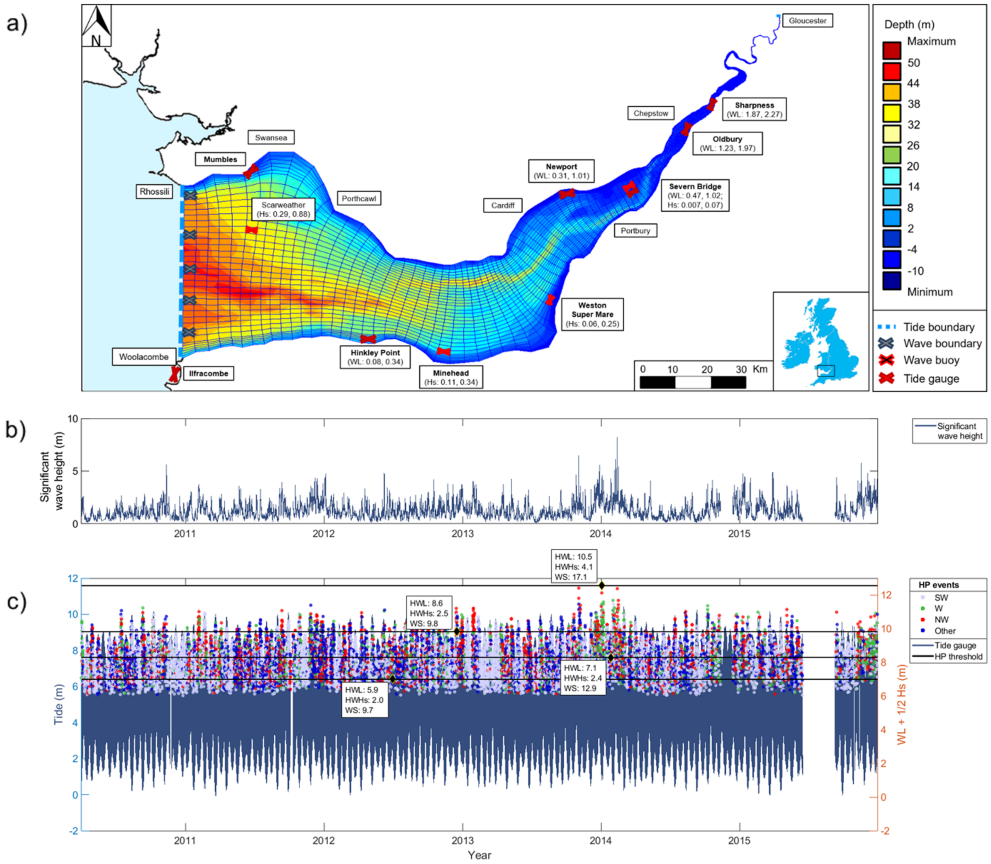

Figure 1. (a) Delft3D-FLOW-WAVE model domain. Bathymetry relative to CD. Average bias and RMSE (m) of WL and H_S model results for four events to tide gauge and wave buoy observations are shown in brackets. (b) Six-year H_S record from Scarweather wave buoy. (c) Long-term tide gauge record taken from Ilfracombe, with HWHP grouped based on wind direction at the time of the event. HWL, HWH_S, and wind speed at the time of the events are shown. Horizontal black lines indicate maximum, 90th, 50th, and 10th percentile HP thresholds.

2. Method

2.1. Delft3D Hindcast of Select Historic Events

The Delft3D modeling system (Lesser et al., 2004) was used to simulate tide-surge-wave propagation across the Severn Estuary for four historic storm events. Delft3D-FLOW simulates hydrodynamic flow under the shallow water assumption, and Delft3D-WAVE simulates the generation and propagation of waves, based on the third-generation spectral wave model Simulating WAves Nearshore, which solves the spectral action balance (Booij et al., 1999). A -2-D horizontal, curvilinear grid of the Severn Estuary extends from Woolacombe, Devon and Rhossili, South Wales in the west, with a maximum resolution of 5 km, to Gloucester in the east with a minimum resolution of 25 m at the coast, to resolve fine-scale processes in shallow water (Figure 1a) and has been validated in Lyddon et al., 2018a, 2018b, 2019. Gridded bathymetry data at 50-m resolution (SeaZone Solutions Ltd., 2013) was interpolated over the 2DH curvilinear grid. Delft3D-FLOW has two open boundaries forced by time varying, spatially uniform water level, representing the Atlantic Ocean to the west and the River Severn to the east. Delft3D-WAVE was forced with five, space-, and time-varying boundary points to the west. Delft3D-WAVE explicitly represents the dissipation of wave energy due to white-capping, bottom friction and depth-induced breaking, and wave generation by wind, and nonlinear wave-wave interactions (Deltares, 2014).

Six years of H_S data from the Scarweather Directional Waverider buoy (Figure 1b) (Cefas, 2018) and tide gauge data at Ilfracombe (NTSLF, 2018) was used to identify historical coastal flood and wave hazard events. H_S was isolated when the tide is at or above 5.91 m (the level of lowest HWL in the record), to leave only wave

events when overtopping is most likely to have occurred (see Figure 1c). This was used to calculate HP for concurrent water level and wave conditions exceeding this threshold (see colored dots in Figure 1c). Each HP event represents a real event with hazard potential and was grouped according to the concurrent wind direction, using data from the Met Office weather station at Pembrey Sands (CEDA, 2018). Winds from a southwest and west direction have been shown to generate maximum H_s and contribute to greatest wave hazard in the estuary (Lyddon et al., 2019). Four events with a southwest and west wind direction were selected, which represent the maximum (3 January 2014, 07:00), 90th (16 December 2012, 19:00), 50th (26 January 2014, 01:00), and 10th percentile (30 June 2012, 12:00) HP thresholds (Figure 1c).

The open sea boundary to the west was forced with a time varying, spatially uniform water level at a 15-min interval using observation data from Ilfracombe tide gauge (NTSLF, 2018). For WAVE standalone simulations, a constant WL was applied at the open sea boundary, at the level of HWL during the selected event, to eliminate the effect of tidal currents on H_s and variability in WL. Time- and space-varying wave conditions (H_s, wave direction, mean period, and directional spread) from the Met Office WAVEWATCH III hindcast (Saulter et al., 2016; Siddorn et al., 2016; Met Office, 2019) were used at five equidistant points along the open sea boundary (see Figure 1a) and were linearly interpolated along the boundary to force the model at 15-min intervals. A time- and space-varying wind and atmospheric pressure field forced the model domain at hourly intervals, using data originating from the Met Office global unified model (Walters et al., 2014) and extracted from the Extended Area Continental Shelf Model CS3X (Williams & Horsburgh, 2013; NOCL, 2019). All simulations were forced with 15-min river gauge data from Sandhurst (Environment Agency, 2016) at an up-estuary open boundary (see Figure 1a).

2.2. Model Validation and Scenario Test

Model outputs from two-way coupling of Delft3D-FLOW-WAVE, which represents a complete five-way multihazard simulation (tide-surge-wind-wave-river), for the four events were validated at five tide gauge locations (Hinkley Point, Newport, Severn Bridge, Oldbury, Sharpness) and four wave buoy locations (Scarweather, Minehead, Weston-super-Mare, Severn Bridge). Average bias and root-mean-square error (RMSE) of WL and H_s were calculated at validation locations (see Figure 1a). The bias is defined as follows:

$$Bias = \overline{M} - \overline{O} \tag{1}$$

where M represents the model values and O the observed values and the overbar denotes the mean value of the simulated storm event. A value of 0 indicates an unbiased estimate; a positive value indicates the model is overpredicting; a negative value is underprediction. The RMSE is defined as follows:

$$RMSE = \sqrt{\overline{(M-O)^2}} \tag{2}$$

where a value closer to 0 indicates better model performance.

There is good agreement for WL in outer estuary. Hinkley Point has a bias value of 0.08 m and RMSE of 0.34 m, which represents 2.75% of the observed tidal range during the maximum event. Positive bias and larger RMSE values up-estuary indicate the model overestimates WL at Oldbury and Sharpness. H_s is well reproduced, as bias and RMSE values remain close to 0. Wave data used for validation are available along the southern estuarine coastline, where areas of critical energy infrastructure are located highlighting the importance of accurately representing H_s in this region.

The validated Delft3D-FLOW and WAVE model was run from 48 hr before the event to 12 hr after, in a series of eight standalone, one-way or two-way coupled simulations. Delft3D-FLOW and WAVE can run in "standalone" mode with user-defined properties (Delft Hydraulics, 2014). Delft3D-WAVE is used in one-way coupled simulations where the FLOW simulation is completed and then input (off-line) into the wave simulation, to account for the effect of flow on waves. Two-way coupled simulations allow dynamic (online) interaction of Delft3D-WAVE with FLOW to account for the effect of waves on current and the effect of current on waves. The FLOW and WAVE modules exchange information at 15-min intervals, such as wave radiation stresses and water level conditions needed for wave transformation, to represent two-way wave-current interaction, refraction and depth-induced breaking. The influence of wind is considered in both FLOW and WAVE when included, to represent changing forcing processes. Eight model runs were

completed for each of the four historical HP events (32 in total) to explore how model coupling and forcing processes contribute to uncertainty in HWL, HWH_s, and HWHP:

Run 1. FLOW
Run 2. FLOW + wind
Run 3. WAVE
Run 4. WAVE + wind
Run 5. FLOW → WAVE (one-way, FLOW output from 1)
Run 6. FLOW → WAVE + wind (one-way, FLOW output from 2)
Run 7. FLOW ←→ WAVE (two-way)
Run 8. FLOW ←→ WAVE + wind (two-way)

The maximum, mean, and median percentage difference in HWL, HWH_s, and HWHP were calculated between each model run and model Run 8 as follows:

$$Percentage\ difference = \frac{(Run\ 8 - Run\ X)}{Run\ 8} \times 100 \quad (3)$$

Run 8 is used as the baseline run as it includes all boundary forcing and has been successfully validated to observational tide and wave data in the estuary. Model results are presented as the % difference between each run and the validated Run 8 for the north and south coastline to (i) identify which coupling HWL, HWH_s, and HWHP are most sensitive to and (ii) quantify uncertainty introduced into the model due to omitting coupling and forcing processes.

3. Results

HWL and HWH_s were extracted from model results every 5 km, from the second row of grid cells in, along the estuary coastline, and HWHP calculated, for each event. Results of the maximum event (3 January 2014) are seen in Figure 2a–2c. HWL (Figure 2a) is amplified to a maximum of 11.7 m up-estuary, beyond Newport and Oldbury, due to the funneling effect (Uncles, 1984). HWH_s (Figure 2b) is greatest in the outer estuary near Swansea and Porthcawl. HWH_s dissipates up-estuary but shows greater sensitivity to coupling and forcing processes. HWHP (Figure 2c) is greatest up-estuary and shows greatest sensitivity to model coupling and forcing in the outer estuary.

The cumulative effect of wave dissipation as energy propagates up-estuary, that is, increased white capping as waves steepen and depth-induced breaking and up-estuary cross-section friction, dampens the hazard; therefore, analyses are focused in areas where water level and waves are largest, in the lower estuary and midestuary. Maximum, mean, and median percentage difference in HWL, HWH_s and HWHP between each run with Run 8 (solid black line in Figures 2a–2c) is calculated for sections of the estuary coastline up to the point where $H_s < 10$ cm in all simulations, termed the wave limit, to focus on the impact on nonnegligible wave conditions (Figures 2d–2f). Absolute differences in HWL, HWH_s and HWHP between each run with run 8 along the coastline are shown in Figures S1a–S1c in the supporting information.

Alongshore maximum, mean, and median % difference relative to Run 8 for HWL, HWH_s, and HWHP are presented for the north (Figure 3a, left panels) and south (Figure 3b, right panels) coastline for each event up to the wave limit ($H_s < 10$ cm), to identify the model's response to coupling processes. Absolute differences in HWL, HWH_s, and HWHP are shown in Figure S2.

3.1. Uncertainty in HWL

Runs 3 and 4 are simulated with a constant water level at MHWST throughout the model domain and no funneling of the tidal wave to amplify tidal range up-estuary occurs (Figure 2a). Up-estuary % difference exceeds 50%; therefore, these are excluded to avoid masking other results. Runs 5 and 6 use the model outputs from Runs 1 and 2 and are excluded to avoid repetition.

The model shows that Runs 1 and 7 generate maximum % difference in HWL along the north and south coastline for all events up to the wave limit, regardless of event severity. Maximum % difference in HWL is 1.5% between Runs 8 and 1 for the 50th percentile event, which also represents maximum absolute difference of 0.046 m (Figure S2a). This absolute difference is <1% of the maximum tidal range. The 90th

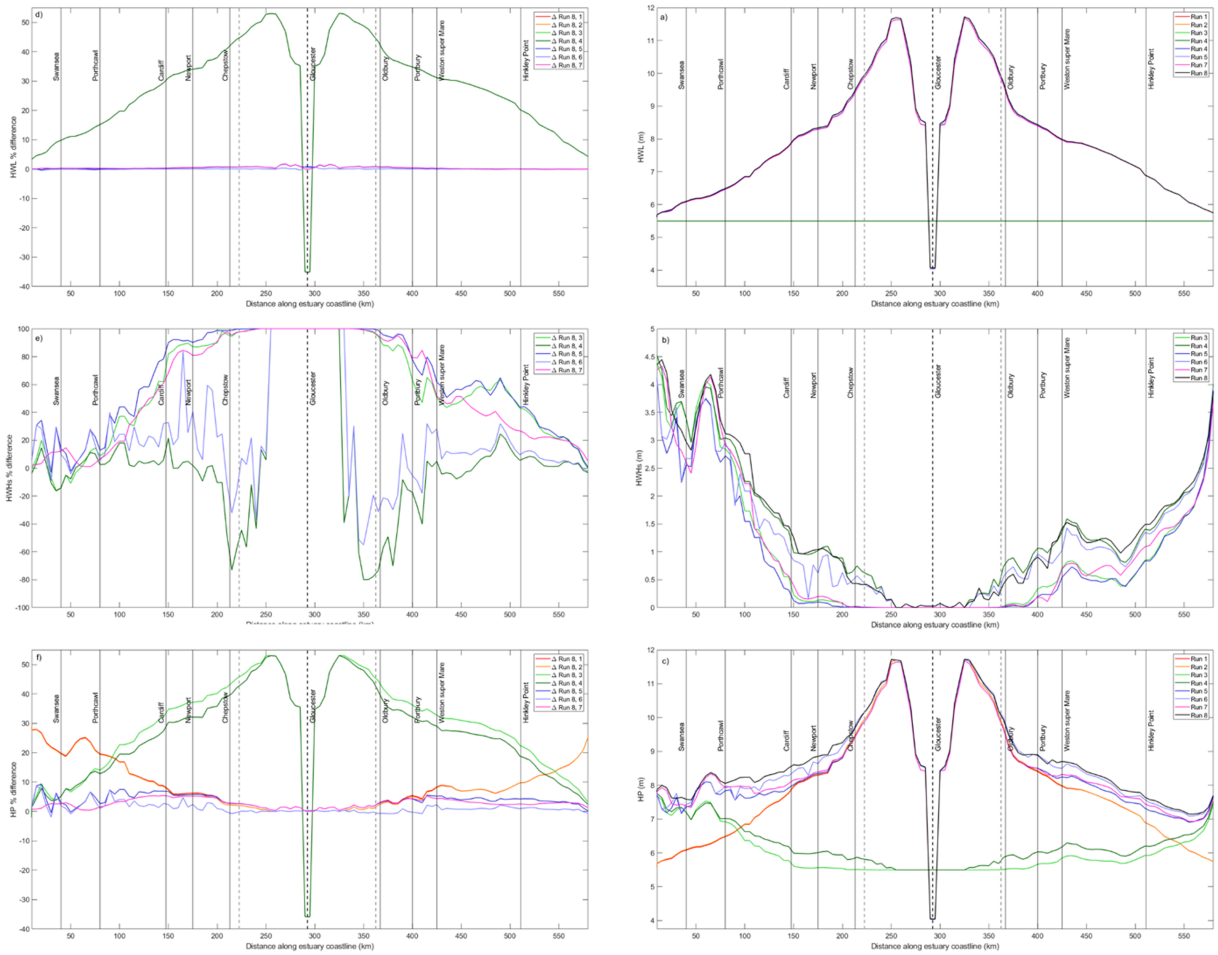

Figure 2. Simulated (a) HWL, (b) HWH_S, and (c) HWHP along the coastline of Severn Estuary starting at Swansea to Gloucester and thence down-estuary toward Woolacombe for maximum event (3 January 2014 07:00); (d–f) % difference between each run and Run 8. The divide between north and south coastlines (dashed black vertical line) and wave limit where $H_S < 10$ cm (dashed gray vertical line) is shown. Solid black vertical lines indicate locations of critical infrastructure and coastal towns.

percentile event shows the least sensitivity to model coupling, where the range in maximum % difference is 0.42% on the north coastline and 0.38% on the south coastline. Run 2 generates the smallest percentage difference in HWL along the north and south coastline for all events, indicating locally generated winds are more important than coupling processes when simulating water level, however, the differences remain small.

3.2. Uncertainty in HWH_S

Increasing HP threshold increases the % and absolute difference in HWH_S on the north coastline, but this trend is less clear on the south coastline. The model highlights up to 90.1% maximum difference in HWH_S 150 km up-estuary, near Cardiff, which represents 1.13 m, between Runs 5 and 8. Figure S3a highlights the substantial % differences in HWH_S up-estuary of the wave limit, and the contribution of local atmospheric forcing to wave generation up-estuary.

The maximum absolute difference in HWH_S is 1.45 m between Runs 5 and 8, which occurs just 20 km up-estuary west of Swansea and represents a 34.4% difference. The geometry of the north coastline means that some stretches of coastline have a more exposed west facing aspect as waves are generated and propagate toward the coast contributing to increased sensitivity to incoming storms with a west-southwest wind direction.

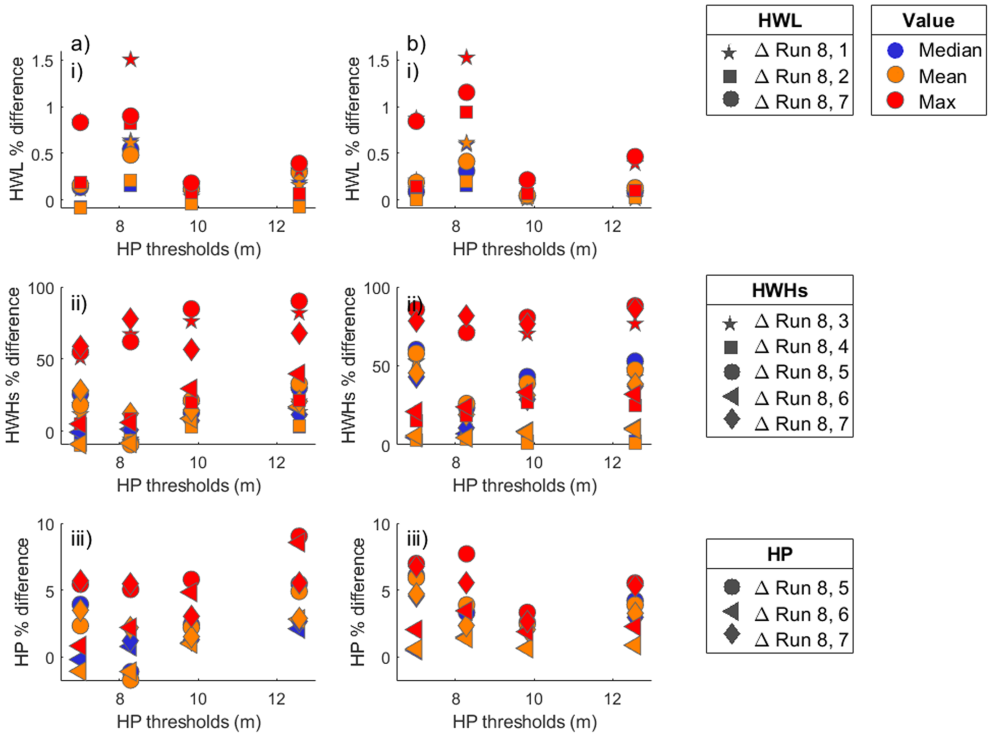

Figure 3. For the (a) north (left panels) and (b) south (right panels) coastlines the alongshore maximum, mean, and median percentage difference in (i) HWL, (ii) HWH_s, and (iii) HWHP between model simulations is calculated for the four events with hazard potential calculated using the HP parameter.

Runs 4 (stand-alone) and 6 (one-way) include local atmospheric forcing and generate a closer representation of HWH_s compared to Run 8, with a 39.9% maximum difference. Runs 4 and 6 generate a range of −9.2% to 17% mean difference for all events. The −51.2% % difference occurs between Runs 8 and 6, which represents 0.48 m, in shallow, sheltered regions (e.g., Swansea Bay and Cardiff Bay) on the north coastline (Figure S1b) where the one-way simulation generates larger HWH_s than two-way simulation. Figure S3b shows one-way simulations underestimate depth-averaged velocities compared to Run 8. HWH_s is overestimated in one-way simulations as slower wave driven currents in shallow areas may mean waves are not refracted around the coastline but instead build in height.

3.3. Uncertainty in HWHP

Runs 1 and 2 are not included in these comparisons as HP is underestimated in the outer estuary when waves are not included as a physical forcing condition (Figure 2f), highlighting the importance of coupling here. Runs 3 and 4are forced with a constant water level and are not included in these comparisons, as HP is greatly underestimated when tide is not included as a physical forcing condition (Figure 2f).

As with HWH_s, increasing HP threshold increases the % and absolute difference in HWHP on the north coastline. Run 5 generates maximum % difference in HWHP of 9.02%, representing 0.71 m, with Run 8 at 20 km up-estuary on the north coastline. The difference between Runs 5 and 8 generates 8.43% difference, 100 km up-estuary on the south coastline; however, this represents just 0.27 m. The south coastline is sheltered from approaching storms simulated here from the southwest, as waves do not propagate directly toward the coastline. Therefore, hazard is lower than the north coastline.

3.4. Spatial Variability of Hazard

Each metric is further analyzed up to the wave limit and the entire estuary, indicating the large impact of model coupling and forcing processes on the upper estuary (Table S1). A greater maximum, mean, and median % difference for HWL and HWH_s occurs when considering the entire estuary coastline. Locally generated winds blow waves into the upper estuary, generating a larger response up-estuary. Conversely, mean

and median % difference for HWHP is smaller when including the upper estuary, and maximum % difference in HWHP occurs in the lower estuary shows no difference.

4. Discussion

The model highlights that HWL shows least sensitivity to forcing and coupling processes. The 90th percentile event, which showed smallest range of % and absolute difference, has a wind speed of 9.8 m/s from 232–247°, representing the most southerly direction of all HP events. This event may be fetch limited, so wind speed is reduced as it approaches from a more southerly direction to reduce setup (Brown et al., 2012), indicating estuary orientation is important when considering uncertainty in simulated HWL at the coastline.

Accurate prediction of HWH_s and HWHP in the outer estuary is important for prediction of wave run-up and wave overtopping and used to design crest levels of flood defense structures (EurOtop, 2018; Sayers et al., 2003). This is particularly important at the time of high tide, when defense exceedance is most likely (Quinn et al., 2014). Largest absolute changes in HWH_s and HWHP occur on sections of the north coastline in the outer estuary with a southwesterly aspect indicating uncertainty, from model and coupling processes, may be sensitive to estuary orientation and coastline geometry in relation to the direction of incoming storm conditions. Accurate model setup for land use planning is critical to avoid underdesign, particularly for infrastructure and communities facing the direction of prevailing storms. Defenses could be built too low if the contribution of local winds to sea generated wave hazard is not considered, leading to more regular, low level "nuisance flooding" (Moftakhari et al., 2018). Future flood damages to coastal cities are estimated at over US$1 trillion damage by the middle of the 21st century (Hallegatte et al., 2013), and this could increase if implementation of new gray or green adaptation strategies are built to inaccurate crest levels and are not able to withstand local storm conditions (Temmerman et al., 2013). At £700–5,400/linear meter for seawalls in the United Kingdom (Hudson et al., 2015) and US$500 million spent annually in the United States on prehazard mitigation (Reguero et al., 2018), over design could be a costly use of funding and resources. Further, a high degree of error in forecasts can propagate through the model cascade (Hewston et al., 2010) when used to then force the boundary of shoreline response models. A 1.45-m underestimation of HWH_s in the outer estuary could mean overtopping models (e.g., EurOtop) or inundation depth and extents (e.g., LISFLOOD-FP) does not accurately capture the impacts of extreme events. This could be costly in terms of management activity or result in financial losses or casualties.

Uncertainty in HWH_s can directly impact on coastal populations up-estuary. HWH_s in Runs 3–7 is consistently smaller than Run 8, as wave propagation may have lost momentum up-estuary due to lack of local wind, or be depth limited (Karimpour et al., 2017). Further, one-way and stand-alone simulations do not account for the effect of waves on current, which may limit wave setup and propagation up-estuary. Increased uncertainty in HWH_s up-estuary of Newport and Weston-super-Mare could underestimate the damaging effects of slopping as a source of coastal flooding (Rego & Li, 2010) or simulated critical threshold levels in operational forecasts may not being reached. Flood warnings may be missed and evacuation orders not sent to coastal communities. This is particularly important in low-lying regions near Oldbury Naite, where simulated HWHP of 9.88 m in Run 8 for the maximum HP event would breach earthen embankments of 9.0 to 9.5 m OD (Knight et al., 2015). Locally generated winds are an important component of operational forecasts in coastal zones, and estuaries to ensure flood warnings are timely and accurate (Marcos et al., 2019).

The importance of locally generated winds in accurate representation of H_s has been shown in coastal and estuarine regions worldwide. Maximum wind speed and surface wind stress are shown to be important in simulating hurricane storm surge with the Sea, Lake, and Overland Surges from Hurricanes model in northeastern United States and can underestimate hazard by 22% if excluded (Mayo & Lin, 2019). The geometry of the mouth of the Mersey Estuary, NW England, at high tide makes it wide enough for substantial local wind-wave generation and for wind setup to elevate the water surface, which should be considered when simulating local flood hazards (Flowerdew et al., 2009). The orientation of hypertidal estuaries to prevailing conditions and their large geometries, such as the Bay of Fundy, Canada, increases the likelihood that strong winds are coincident with extreme total water levels (Desplanque & Mossman, 1999). Simulated H_s during the Patriot's Day storm in the Bay of Fundy show maximum H_s occurs in the outer Gulf of Maine due to long fetch and wind setup (Marsooli & Lin, 2018), indicating the importance of local winds during extreme storm

events. Storm surges are often accompanied by large wind waves in more than half of coastal regions worldwide (Marcos et al., 2019), thus increasing the potential for coastal flooding and highlighting the need for accurate, local boundary conditions when simulating HWH_s.

5. Conclusion

Potential future changes in sea level and storm tracks necessitate accurate prediction of HWL and HWH_s in hypertidal coastal and estuarine areas for operational forecasts, inundation assessments and cost-effective defense strategies. Delft3D-FLOW-WAVE is used in a series of 32 stand-alone, one-way or two-way coupled simulations for four historic storm events, to quantify the uncertainty in forecasting HWL and HWH_s due to coupling and forcing processes in the Severn Estuary, SW England, used here as a test case for hypertidal and funnel shaped estuaries worldwide. HWL shows least sensitivity to both coupling and forcing processes, with 1.5% difference (0.046 m) between the two-way coupled and standalone simulation. For a model domain this size, inclusion of local atmospheric forcing is crucial to continue to add momentum to wave generation up-estuary for accurate HWH_s and HWHP prediction. The model shows a 34.4% difference (1.45 m) in HWH_s and 9.02% (0.71 m) in HWHP on the north shoreline in the outer estuary and up to 90.1% difference (1.13 m) in the upper estuary when local atmospheric forcing is excluded from simulations. Aspect and geometry of the coastline to prevailing storm conditions is also an important consideration for coastal hazard prediction. Results highlight how coastal and estuarine numerical models can be best set up to ensure outputs can be used in confidence to force shoreline response models (e.g., for overtopping or inundation studies), to inform design of new coastal protection schemes or flood warnings.

Acknowledgments
The authors thank colleagues at the British Oceanographic Data Centre (BODC) for providing tidal data, Magnox for providing tidal data, Environment Agency for providing tidal data, Gloucester Harbour Trustees for providing tidal data, Met Office for providing observational wind data and WAVEWATCH III data, Met Office and NOCL for providing CS3X wind and atmospheric pressure data, CEFAS for providing observational wave buoy data, and EDINA for providing bathymetric data. The research is a contribution to the Natural Environment Research Council UK highlight topic "Physical and biological dynamic coastal processes and their role in coastal recovery" (BLUE-coast, NE/N015614/1). Data used in this research are available from sources stated in the reference list.

References

Barnard, P. L., Erikson, L. H., Foxgrover, A. C., Hart, J. A. F., Limber, P., O'Neill, A. C., et al. (2019). Dynamic flood modeling essential to assess the coastal impacts of climate change. *Scientific Reports*, *9*(1), 1, 4309–13. https://doi.org/10.1038/s41598-019-40742-z

Bolaños, R., Brown, J. M., & Souza, A. J. (2014). Wave-current interactions in a tide dominated estuary. *Continental Shelf Research*, *87*, 109–123. https://doi.org/10.1016/j.csr.2014.05.009

Booij, N., Ris, R. C., & Holthuijsen, L. H. (1999). A third-generation wave model for coastal regions 1. Model description and validation. *Journal of Geophysical Research*, *104*(C4), 7649–7666.

Brown, J. M., Bolaños, R., Howarth, M. J., & Souza, A. J. (2012). Extracting sea level residual in tidally dominated estuarine environments. *Ocean Dynamics*, *62*(7), 969–982. https://doi.org/10.1007/s10236-012-0543-7

Cefas (2018). WaveNet Data download [online] Available at: http://wavenet.cefas.co.uk/Map [].

Centre for Environmental Data Analysis (2018). Met Office Integrated Data Archive System (MIDAS) Land and Marine Surface Stations Data [online] Available at: http://catalogue.ceda.ac.uk/ [].

Conger, T., & Chang, S. E. (2019). Developing indicators to identify coastal green infrastructure potential: The case of the Salish Sea region. *Ocean and Coastal Management*, *175*(February), 53–69. https://doi.org/10.1016/j.ocecoaman.2019.03.011

Del Río, L., Plomaritis, T. A., Benavente, J., Valladares, M., & Ribera, P. (2012). Establishing storm thresholds for the Spanish Gulf of Cádiz coast. *Geomorphology*, *143–144*, 13–23. https://doi.org/10.1016/j.geomorph.2011.04.048

Delft Hydraulics. (2014). *Delft3D-WAVE. Simulations of short crested waves with SWAN Version 3.05, Revision 34160*. Deltares, 2600 MH Delft, The Netherlands.

Deltares. (2014). *Delft3D-WAVE*. 1–226.

Desplanque, C., & Mossman, D. J. (1999). Storm tides of the Fundy. *American Geographical Society*, *89*(1), 23–33.

Dyer, K. R. (1995). Chapter 14: Sediment transport in estuaries. In *Geomorphology and sedimentology of estuaries: Developments in Sedimentology* (pp. 423–449). New York: Elsevier.

Environment Agency (2016). River Severn hourly water level data, Sandhurst gauge, shwgenquiries@environment-agency.gov.uk.

Environment Agency. (2018). New £63 million defence scheme is turning the tide against floods in Rossall. Retrieved May 9, 2019, from Gov.uk website: https://www.gov.uk/government/news/new-63-million-defence-scheme-is-turning-the-tide-against-floods-in-rossall

EurOtop. (2018). Manual on wave overtopping of sea defences and related structures: second edition.

Fairclough, I. (2019). Province, Ottawa spending $114m to reinforce Bay of Fundy dikes against rising seas. Retrieved May 8, 2019, from The Chronicle Herald website: https://www.thechronicleherald.ca/news/local/province-ottawa-spending-114m-to-reinforce-bay-of-fundy-dykes-against-rising-seas-302999/

Flowerdew, J., Hawkes, P., Mylne, K., Pullen, T., Saulter, A., & Tozer, N. (2009). *Coastal flood forecasting: Model development and evaluation*. Bristol: Environment Agency.

Greenberg, D. A., Blanchard, W., Smith, B., & Barrow, E. (2012). Climate change, mean sea level and high tides in the Bay of Fundy. *Atmosphere-Ocean*, *50*(3), 261–276. https://doi.org/10.1080/07055900.2012.668670

Hallegatte, S., Green, C., Nicholls, R. J., & Corfee-Morlot, J. (2013). Future flood losses in major coastal cities. *Nature Climate Change*, *3*(9), 802–806. https://doi.org/10.1038/nclimate1979

Hewston, R., Chen, Y., Pan, S., Zou, Q., Reeve, D., & Cluckie, I. D. (2010). Quantifying uncertainty in tide, surge and wave modelling during extreme storms. *BHS Third International Symposium, Managing Consequences of a Changing Global Environment*, (January 2015). https://doi.org/10.7558/bhs.2010.ic74

Hudson, T., Keating, K., Petit, A., Chatterton, J., & Williams, A. (2015). Cost estimation for coastal protection - summary of evidence. Retrieved from www.environment-agency.gov.uk%0Awww.gov.uk/government/publications.

Karimpour, A., Chen, Q., & Twilley, R. R. (2017). Wind wave behavior in fetch and depth limited estuaries. *Nature Scientific Reports*, *7*(1), 1–8. https://doi.org/10.1038/srep40654

Knight, P. J., Prime, T., Brown, J. M., Morrissey, K., & Plater, A. J. (2015). Application of flood risk modelling in a web-based geospatial decision support tool for coastal adaptation to climate change. *Natural Hazards and Earth System Sciences*, *15*(7), 1457–1471. https://doi.org/10.5194/nhess-15-1457-2015

Lawless, M., Hird, M., Rodger, D., Gouldby, B., Tozer, N., Pullen, T., et al. (2016). *Investigating coastal flood forecasting Good practice framework*. Bristol: Environment Agency.

Lesser, G. R., Roelvink, J. A., van Kester, J. A. T. M., & Stelling, G. S. (2004). Development and validation of a three-dimensional morphological model. *Coastal Engineering*, *51*(8–9), 883–915. https://doi.org/10.1016/j.coastaleng.2004.07.014

Lyddon, C., Brown, J. M., Leonardi, N., & Plater, A. J. (2018a). Flood hazard assessment for a hyper-tidal estuary as a function of tide-surge-morphology interaction. *Estuaries and Coasts*, *41*(6), 1565–1586. https://doi.org/10.1007/s12237-018-0384-9

Lyddon, C., Brown, J. M., Leonardi, N., & Plater, A. J. (2018b). Uncertainty in estuarine extreme water level predictions due to surge-tide interaction. *PLoS ONE*, *13*(10), 1–17. https://doi.org/10.1371/journal.pone.0206200

Lyddon, C. E., Brown, J. M., Leonardi, N., & Plater, A. J. (2019). Increased coastal wave hazard generated by differential wind and wave direction in hyper-tidal estuaries. *Estuarine, Coastal and Shelf Science*, *220*, 131–141. https://doi.org/10.1016/j.ecss.2019.02.042

Marcos, M., Rohmer, J., Vousdoukas, M., Mentaschi, L., Le Cozannet, G., & Amores, A. (2019). Increased extreme coastal water levels due to the combined action of storm surges and wind-waves. *Geophysical Research Letters*, *46*(8), 4356–4364. https://doi.org/10.1029/2019GL082599

Marsooli, R., & Lin, N. (2018). Numerical modeling of historical storm tides and waves and their interactions along the U.S. East and Gulf Coasts. *Journal of Geophysical Research: Oceans*, *123*(5), 3844–3874. https://doi.org/10.1029/2017JC013434

Mayo, T., & Lin, N. (2019). The effect of the surface wind field representation in the operational storm surge model of the National Hurricane Center. *Atmosphere*, *10*(4), 193. https://doi.org/10.3390/atmos10040193

Met Office (2019). Hindcast WAVEWATCH III model wave data at grid points 51.217 N 4.240 W, 51.927 N 4.243 W, 51.377 N 4.246 W, 51.457 N 4.250 W, 51.537 N 4.252 W.

Moftakhari, H. R., AghaKouchak, A., Sanders, B. F., Allaire, M., & Matthew, R. A. (2018). What is nuisance flooding? Defining and monitoring an emerging challenge. *Water Resources Research*, *54*(7), 4218–4227. https://doi.org/10.1029/2018WR022828

NOCL (National Oceanography Centre Liverpol) (2019). CS3X hindcast wind and atmospheric pressure model data.

NTSLF (National Tidal and Sea Level Facility) (2018). UK Tide Gauge Network [online] Available at: https://www.bodc.ac.uk/data/hosted_data_systems/sea_level/uk_tide_gauge_network/

O'Neill, C., Saulter, A., Williams, J., & Horsburgh, K. (2016). NEMO-surge: Application of atmospheric forcing and surge evaluation. Technical report 619.

Pye, K., & Blott, S. J. (2010). A consideration of "extreme events" at Hinkley Point. *Tecnhical Report Series*, *2010*(109), 57.

Quinn, N., Lewis, M., Wadey, M. P., & Haigh, I. D. (2014). Assessing the temporal variability in extreme storm-tide time series for coastal flood risk assessment. *Journal of Geophysical Research: Oceans*, *119*, 2227–2237. https://doi.org/10.1002/2013JC009305.Received

Rego, J. L., & Li, C. (2010). Nonlinear terms in storm surge predictions: Effect of tide and shelf geometry with case study from Hurricane Rita. *Journal of Geophysical Research*, *115*, C005285. https://doi.org/10.1029/2009JC005285

Reguero, B. G., Beck, M. W., Bresch, D. N., Calil, J., & Meliane, I. (2018). Comparing the cost effectiveness of nature-based and coastal adaptation: A case study from the Gulf Coast of the United States. *PLoS ONE*, *13*(4), 1–24. https://doi.org/10.1371/journal.pone.0192132

Saulter, A., Bunney, C., & Li, J. (2016). Application of a refined grid global model for operational wave forecasting.

Sayers, P., Gouldby, B., Simm, J., Meadowcroft, I., & Hall, J. (2003). Risk, performance and uncertainty in flood and coastal defence—A review. *R&D Technical Report FD2302/TR1. HR Wallingford*, 115.

SeaZone Solutions Ltd. (2013). Gridded bathymetry: 1 Arcsecond [ascii], Scale 1:50,000, Tile: NW 55050025, NW 55050030, NW 55050035, NW 55050040, NW 55050045, NW 55100030, NW, 5100035, NW 55100040, NW 55100045, NW 55150025, NW 55150030, NW 55150035, NW 55150040, NW 55150045, Updated August 2013, Crown Copyright/SeaZone Solutions Ltd., UK. Using: EDINA Marine Digimap Service, http://edina.ac.uk/digimap, [Accessed January 2016].

Sibley, A., Cox, D., & Titley, H. (2015). Coastal flooding in England and Wales from Atlantic and North Sea storms during the 2013/2014 winter. *Weather*, *70*(2), 62–70.

Siddorn, J. R., Good, S. A., Harris, C. M., Lewis, H. W., Maksymczuk, J., Martin, M. J., & Saulter, A. (2016). Research priorities in support of ocean monitoring and forecasting at the Met Office. *Ocean Science*, *12*(1), 217–231. https://doi.org/10.5194/os-12-217-2016

Stephens, S., Bell, R., & Lawrence, J. (2017). Applying principles of uncertainty within coastal hazard assessments to better support coastal adaptation. *Journal of Marine Science and Engineering*, *5*(3), 40. https://doi.org/10.3390/jmse5030040

Temmerman, S., Meire, P., Bouma, T. J., Herman, P. M. J., Ysebaert, T., & De Vriend, H. J. (2013). Ecosystem-based coastal defence in the face of global change. *Nature*, *504*(7478), 79–83. https://doi.org/10.1038/nature12859

Tunstall, S., Johnson, C. L., & Rowsell, E. C. P. (2004). Flood hazard management in England and Wales: From land drainage to flood risk management. *World Congress on Natural Disaster Mitigation*, (February), 1–8.

Uncles, R. J. (1984). Hydrodynamics of the Bristol Channel. *Marine Pollution Bulletin*, *15*(2), 47–53. https://doi.org/10.1016/0025-326X(84)90461-2

Walters, D. N., Williams, K. D., Boutle, I. A., Bushell, A. C., Edwards, J. M., Field, P. R., et al. (2014). The Met Office Unified Model Global Atmosphere 4.0 and JULES Global Land 4.0 configurations. *Geoscientific Model Development*, *7*(1), 361–386. https://doi.org/10.5194/gmd-7-361-2014

Williams, J. A., & Horsburgh, K. J. (2013). Evaluation and Comparison of the operational Bristol Channel Model storm surge suite. *NOC Research and Consultancy Report*. https://doi.org/10.1007/s13398-014-0173-7.2

Wolf, J. (2009). Coastal flooding: Impacts of coupled wave-surge-tide models. *Natural Hazards*, *49*(2), 241–260. https://doi.org/10.1007/s11069-008-9316-5

Yin, K., Xu, S., Huang, W., & Xie, Y. (2017). Effects of sea level rise and typhoon intensity on storm surge and waves in Pearl River Estuary. *Ocean Engineering*, *136*, 80–93. https://doi.org/10.1016/j.oceaneng.2017.03.016